

Risk of the hydrogen economy for atmospheric methane

Original

Risk of the hydrogen economy for atmospheric methane / Bertagni, M. B.; Pacala, S. W.; Paulot, F.; Porporato, A.. - In: NATURE COMMUNICATIONS. - ISSN 2041-1723. - 13:1(2022). [10.1038/s41467-022-35419-7]

Availability:

This version is available at: 11583/2994884 since: 2024-11-29T10:05:09Z

Publisher:

Nature Research

Published

DOI:10.1038/s41467-022-35419-7

Terms of use:

This article is made available under terms and conditions as specified in the corresponding bibliographic description in the repository

Publisher copyright

(Article begins on next page)

Risk of the hydrogen economy for atmospheric methane

Received: 5 April 2022

Accepted: 24 November 2022

Published online: 13 December 2022

 Check for updatesMatteo B. Bertagni¹✉, Stephen W. Pacala², Fabien Paulot³ & Amilcare Porporato^{1,4}

Hydrogen (H₂) is expected to play a crucial role in reducing greenhouse gas emissions. However, hydrogen losses to the atmosphere impact atmospheric chemistry, including positive feedback on methane (CH₄), the second most important greenhouse gas. Here we investigate through a minimalist model the response of atmospheric methane to fossil fuel displacement by hydrogen. We find that CH₄ concentration may increase or decrease depending on the amount of hydrogen lost to the atmosphere and the methane emissions associated with hydrogen production. Green H₂ can mitigate atmospheric methane if hydrogen losses throughout the value chain are below $9 \pm 3\%$. Blue H₂ can reduce methane emissions only if methane losses are below 1%. We address and discuss the main uncertainties in our results and the implications for the decarbonization of the energy sector.

Commitments to reach net-zero carbon emissions have drawn renewed attention to hydrogen (H₂) as a low-carbon energy carrier^{1,2}. Currently, H₂ is mostly used as an industrial feedstock, and its global production has a high carbon footprint because it relies almost entirely ($\approx 95\%$) on fossil fuels¹. However, many technologies to produce H₂ with a lower carbon footprint are available¹. Among these, low-carbon H₂ can be produced from water electrolysis powered by renewable energy (green H₂) or from methane reforming coupled with carbon capture and storage (blue H₂). H₂ fuel may be especially important to decarbonize energy and transport sectors where direct electrification is complicated, like heavy industry, heavy-duty road transport, shipping, and aviation¹. H₂ is also being considered for storing renewable energy¹. As a result of this potential, countries accounting for more than a third of the world's population have developed national strategies for large-scale H₂ production^{1,2}.

Even if a more hydrogen-based economy would reduce CO₂ emissions and improve air quality³, it would also increase the H₂ emissions into the atmosphere. The H₂ molecule is very small and difficult to contain, so it is still largely unknown how much H₂ will leak in future value chains. H₂ emissions will also occur due to venting, purging, and incomplete combustion^{4–6}. This potential increase in H₂

emissions has received relatively little attention to date because H₂ is neither a pollutant nor a greenhouse gas (GHG). However, it has been long known^{7–10} that H₂ emissions may exert a significant indirect radiative forcing by perturbing the concentration of other GHG gases in the atmosphere. This indirect GHG effect of H₂ calls for a detailed scrutiny of the global H₂ budget and the environmental consequences of its perturbation^{11,12}.

H₂ is the second most abundant reactive trace gas in the atmosphere, after methane, with an average concentration of around 530 ppb_v¹³. H₂ sources include both direct emissions ($\approx 45\%$ of total sources) and production in the troposphere from the oxidation of volatile organic compounds ($\approx 25\%$) and methane ($\approx 30\%$)^{11,14}. The main H₂ sinks are the uptake by soil bacteria (70–80% of total tropospheric removal) and the atmospheric reaction with the radical OH (20–30%), which is responsible for the indirect GHG effect of H₂. H₂'s reaction with the OH radical tends to increase tropospheric methane (CH₄) and ozone (O₃), which are two potent greenhouse gases. It also increases stratospheric water vapor, which is associated with stratospheric cooling and tropospheric warming^{8,15}. Recent global climate models have estimated that hydrogen has an indirect radiative forcing of around $1.3^{14}–1.8^{16} \cdot 10^{-4} \text{ W m}^{-2} \text{ ppb}_v^{-1}$, and a global warming potential (GWP) that lies in the

¹The High Meadows Environmental Institute, Princeton University, Guyot Hall, Princeton 08544 NJ, USA. ²Department of Ecology and Evolutionary Biology, Princeton University, Guyot Hall, Princeton 08544 NJ, USA. ³Geophysical Fluid Dynamics Laboratory, National Oceanic and Atmospheric Administration, 201 Forrestal Rd, Princeton 08540 NJ, USA. ⁴Department of Civil and Environmental Engineering, Princeton University, Guyot Hall, Princeton 08544 NJ, USA.

✉ e-mail: matteobb@princeton.edu

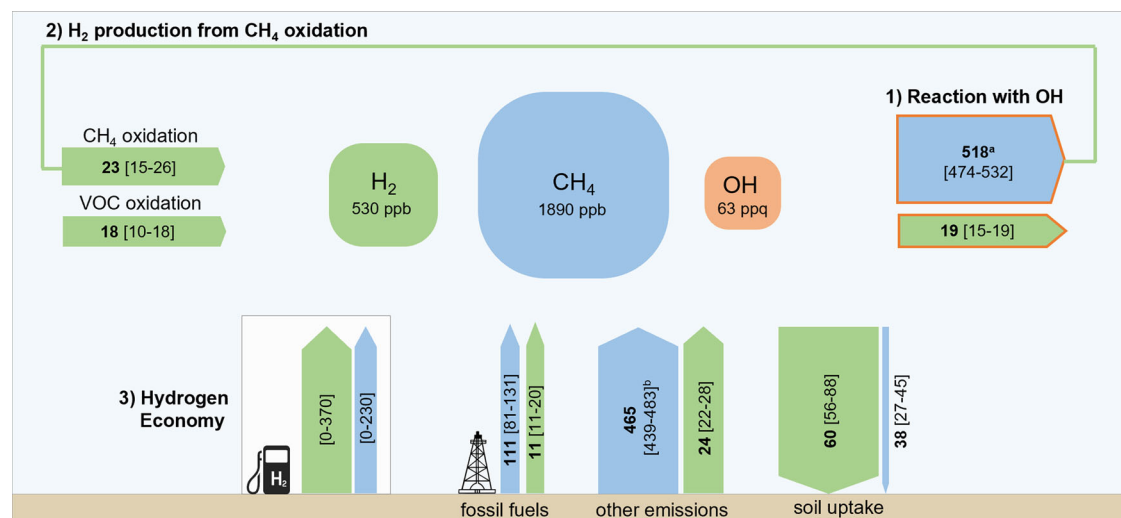


Fig. 1 | Tangled hydrogen (H₂) and methane (CH₄) budgets. Sketch of H₂ and CH₄ tropospheric budgets and their interconnections: (1) the competition for OH; (2) the production of H₂ from CH₄ oxidation; (3) the potential emissions [minimum-maximum] due to a more hydrogen-based energy system. Flux estimates (Tg/year) are from refs. 11,18. Arrows are scaled with mass flux intensity, CH₄ scale being 10

times narrower than H₂ scale. On a per-mole basis, H₂ consumes only around 3 times less OH than CH₄. ppq = part per quadrillion (10⁻¹⁵). ^a top-down estimate including also minor atmospheric sinks (<10%). ^b range obtained as a difference between total and fossil fuel emissions¹⁸.

range 11 ± 5 for a 100-year time horizon¹⁶. Hence, H₂ emissions are far from being climate neutral, and their largest impact is related to the perturbation of atmospheric CH₄^{14,16}, the second most important anthropogenic GHG.

The tropospheric budgets of H₂ and CH₄ are deeply interconnected (Fig. 1). First, the removal of both gases from the atmosphere is controlled by their reaction with OH, which is the dominant sink ($\approx 90\%$) for atmospheric methane^{17,18}. An increase in the concentration of tropospheric H₂ may reduce the availability of OH, consequently weakening CH₄'s removal and increasing CH₄'s lifetime and abundance^{14,19}. Second, methane is a primary precursor of hydrogen. Namely, CH₄ oxidation results in the production of formaldehyde, whose photolysis produces H₂. Firm-air records suggest that the increase in H₂ over the 20th century can be largely explained by the increase in CH₄ concentration²⁰.

Additionally, H₂ and CH₄ are linked at the industrial level. Around 60% of global H₂ production is currently produced from steam methane reforming (gray H₂) and is responsible for 6% of global natural gas use¹. In the next decade, steam methane reforming coupled with carbon capture and storage will likely remain the dominant technology for large-scale H₂ production (blue H₂), since facilities for H₂ production from renewable sources (green H₂) will require time to become operational and economically favorable².

Since CH₄ is the second-largest contributor to atmospheric warming since the beginning of the industrial era and there are global efforts to mitigate its atmospheric levels²¹, it is crucial to quantify the response of atmospheric CH₄ to increasing H₂ production.

We analyze this problem through a simple atmospheric model that captures the interaction between H₂ and CH₄ ("Methods"). The investigation of the transient dynamics ("Methods") shows that any H₂ emissions pulse to the atmosphere leads to a small transient growth of atmospheric CH₄ whose effects last for several decades. In the next sections, we focus on how the equilibrium concentrations of tropospheric H₂ and CH₄ would respond to scenarios of continuous emissions from an energy system where part of the fossil fuel energy share is replaced by green or blue H₂. The analysis emphasizes how atmospheric CH₄ could either decrease or increase, mainly depending on the H₂ production pathway and the amount of H₂ lost to the atmosphere. The latter is defined through the hydrogen emission intensity (HEI), namely the percentage of H₂ produced that is lost to the

atmosphere. Specifically, we find a critical HEI above which the CH₄ atmospheric burden rises despite the lower fossil fuel use. We assess the critical factors and the main uncertainties in the quantification of this critical HEI. We finally discuss how our results can help better inform policymakers regarding the trade-off associated with different scenarios of hydrogen production and use.

Results

Emission scenarios

Here we investigate how the tropospheric burdens of methane and hydrogen would be affected by the transition to a more hydrogen-based energy system, wherein hydrogen replaces part of the current fossil fuel energy (≈ 490 ExJ in 2019²²). To achieve this goal, we estimate the CH₄ and H₂ source changes, ΔS_{CH_4} and ΔS_{H_2} , where Δ indicates the difference to the current tropospheric conditions ("Methods"). This fossil fuel displacement reduces both CH₄ and H₂ sources (Fig. 1). The rise in H₂ production causes additional H₂ emissions due to intentional (e.g., venting) and unintended (e.g., fugitive) losses, and possibly CH₄ emissions associated with blue H₂ production.

The change in H₂ emissions can be estimated from the amount of hydrogen produced to substitute fossil fuels and the HEI, namely the percentage of H₂ produced that is lost to the atmosphere. Losses can occur due to venting, purging, incomplete combustion and leaks across the hydrogen value chain. The HEI of the future global H₂ value chain is very uncertain. Literature values range from 1 to 12%^{4,9,23}, but the upper bound is unlikely to occur at large scales because it would be both unsafe and too expensive. Recent empirical estimates for specific H₂ infrastructures suggest HEI's ranging from 0.1 to 6.9%, critically depending on the pathway of hydrogen production and transport⁶. To account for these uncertainties and to explore a broad spectrum of possible scenarios, here we vary HEI from 0 to 10% of the total hydrogen produced (Fig. 2a). The lower and upper bounds of this range represent a perfectly sealed and a highly leaking global H₂ value chain, respectively. With a perfectly sealed hydrogen value chain, H₂ emissions would only decrease due to the lower fossil fuel use. On the contrary, a highly leaking H₂ value chain, coupled with an envisioned penetration of H₂ in the energy market, could increase hydrogen emissions up to several times the total current sources, which are around 80 Tg H₂ yr⁻¹.

The variation in CH₄ emissions depends not only on the percentage of fossil fuel energy that is displaced by hydrogen, but also on the

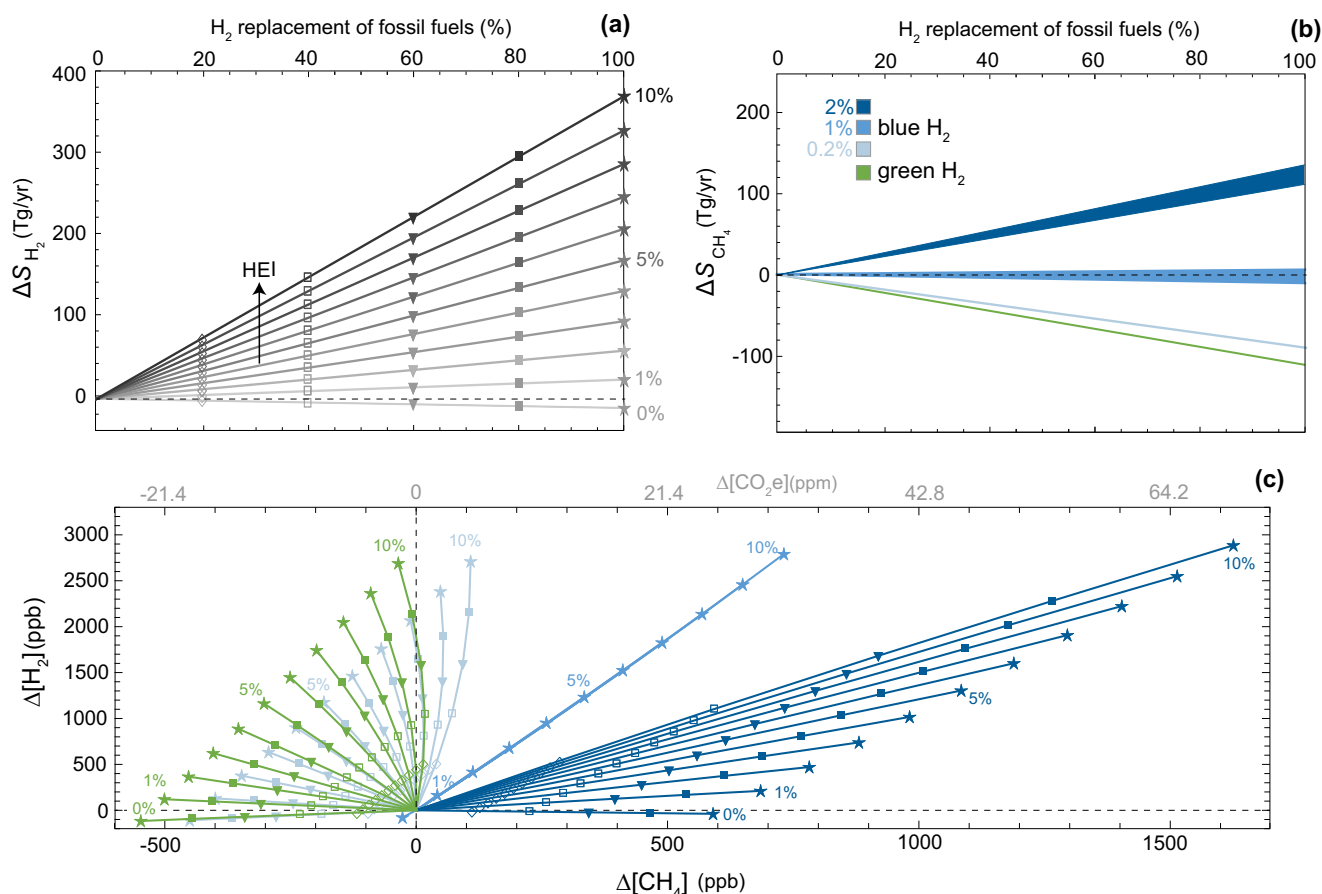


Fig. 2 | Hydrogen replacement of fossil fuels. a Changes in H₂ sources (ΔS_{H_2}) as a function of fossil fuel replacement for different hydrogen emission intensity (HEI). **b** Changes in CH₄ sources (ΔS_{CH_4}) as a function of fossil fuel replacement for different H₂ production pathways. Methane leak rates associated with blue H₂ production are 0.2, 1, and 2%. Bands for ΔS_{CH_4} account for different amounts of blue H₂ produced and lost. **c** Response of the tropospheric concentrations of H₂

and CH₄ for the emission scenarios of the previous panels. Symbols mark the different percentages of fossil fuel displacement. Only symbols for 100% fossil fuel replacement are reported for blue H₂ with 1% CH₄ leakage. Also reported is the difference in CO₂ concentration ($\Delta[CO_2e]$) that would produce equivalent radiative forcing to the change in equilibrium CH₄ (upper axis).

hydrogen production pathway. For green H₂, i.e., hydrogen obtained from renewable sources, we scale CH₄ emissions based on the reduced consumption of fossil fuels resulting from hydrogen usage (Fig. 2b). Estimates of current methane emissions associated with fossil fuel extraction and distribution are in the range 80–160 Tg CH₄ yr⁻¹^{18,24,25} and relatively equally distributed among coal, oil, and gas sectors²⁶. Here we use the top-down estimate of 111 Tg/year¹⁸.

For blue H₂, which is derived from steam methane reforming (SMR), the variation in CH₄ sources not only accounts for the reduced consumption of fossil fuels but also for the methane emissions (venting, incomplete combustion, fugitive) associated with blue hydrogen production. These emissions depend on the amount of CH₄ needed to produce H₂, i.e., feedstock and energy requirements of the SMR process (“Methods”), and the CH₄ leak rate. The precise average leak rate of the global natural gas supply chain remains uncertain. One of the reasons is that national inventories generally underestimate real emissions^{27–30}. More detailed studies relying on field measurements in the United States and Canada estimate average leak rates around 2%^{28–30}, with large spatial heterogeneity between different operators³¹. Although national inventories suggest that some countries, like Venezuela and Turkmenistan, have higher leak rates²⁶, here we adopt 2% as the maximum global CH₄ leak rate for our scenarios, because methane-mitigation efforts are likely to decrease future global leak rates³¹ and, more importantly, because not all hydrogen produced will be blue H₂. In this regard, the scenario of blue H₂ with a 2% CH₄ leak rate can also be interpreted as a combination of equal production of

green H₂ and blue H₂ with 4% CH₄ leak rate. We use 0.2% as a lower bound for the CH₄ leak rate, since this has been declared as the target of several energy companies for 2025³². 1% represents an intermediate scenario of blue H₂ production.

Figure 2b shows the resulting CH₄ emissions associated with green and blue H₂ production with methane leak rates of 0.2, 1, and 2%. The different leak rates have a great impact on the methane emissions. Compared to the fossil fuel energy system, CH₄ emissions are reduced in the blue H₂ scenario with 0.2% methane losses, but largely increased in the blue H₂ scenario with 2% methane losses. The fossil fuel displacement by blue H₂ with 1% methane losses shows basically no net effect on the CH₄ emissions.

As a specific case, we also investigate the H₂ and CH₄ emission changes associated with estimates of future hydrogen production in a set of net-zero scenarios. H₂ production is expected to increase from current 90 Tg/year to 530–660 Tg/year in 2050^{2,33,34}. We thus consider a 500 Tg/year rise in the global H₂ production, which is energetically equivalent to about 15% of current fossil fuel energy. Figure 3a shows how, depending on the H₂ production pathway and the different hydrogen and methane leak rates, the emission changes of these two gases can vary substantially.

Tropospheric response

For the previous emission scenarios, we evaluate the changes in the equilibrium concentrations of tropospheric hydrogen and methane, namely $\Delta[H_2]$ and $\Delta[CH_4]$. The timescales to equilibrium are dictated

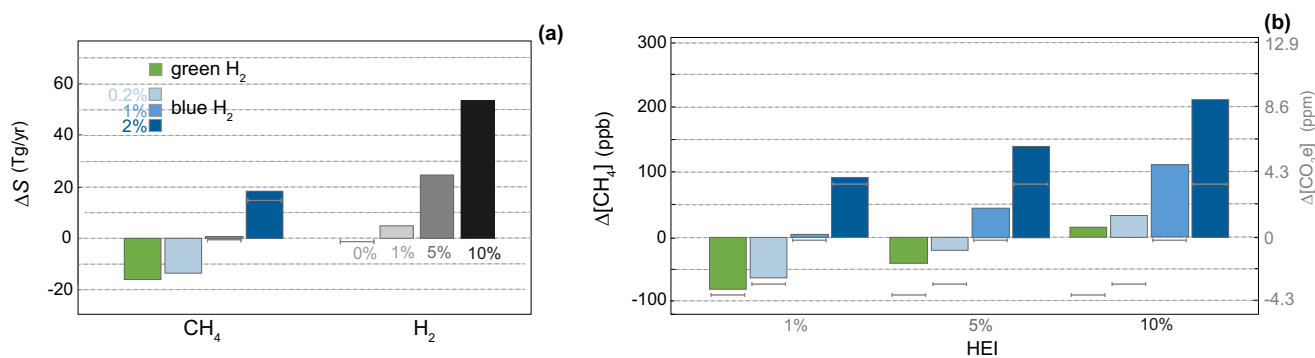


Fig. 3 | Methane response to increasing H₂ production. a Changes in H₂ and CH₄ sources (ΔS) due to green and blue H₂ production (≈500 Tg yr⁻¹). HEI is the H₂ emission intensity. Gray lines mark the case for HEI = 0%. Blue bars for ΔS_{CH₄} are

obtained with HEI = 10%. **b** Response of CH₄ atmospheric concentration. The right axis shows the Δ[CO₂e] that would produce equivalent radiative forcing to the change in equilibrium CH₄.

by the gas average lifetimes (“Methods”). The corresponding variations in steady state concentration of OH are reported in Supplementary Figs. 1 and 2.

The H₂ economy causes a rise in tropospheric H₂ as a result of the additional emissions (Fig. 2c). The intensity of this increase varies considerably as a function of the emissions of the hydrogen value chain. The concentration variation could go from less than 100 ppb_v to more than 2000 ppb in envisioned scenarios of the H₂ economy, namely a +300% from the current H₂ tropospheric level.

The response of atmospheric CH₄ results from the combination of the methane emission change and the methane sink weakening due to the higher hydrogen emissions. To discriminate between the two mechanisms, it is useful to focus on the scenarios of fossil fuel displacement by green H₂. In the case of a perfectly sealed green H₂ value chain (HEI = 0%), [CH₄] and [H₂] both decrease due to reduction in fossil fuel emissions. As H₂ emissions increase (HEI > 0), Δ[CH₄] increases too. Up to the point that when HEI overcomes a critical threshold, there is an increase in atmospheric methane, i.e., Δ[CH₄] > 0, even though methane emissions are lower. This critical HEI is in the range 8–10% for green H₂ as it has a weak nonlinear dependence on the percentage of fossil fuel energy that is replaced by H₂ (see also Supplementary Fig. 3).

The scenarios of blue H₂ with 0.2% CH₄ leak rates are not very different from the green H₂ scenarios, with the critical HEI being in the range 7–8%. Regarding the scenarios of blue H₂ with 1% CH₄ leak rates, since there is basically no change in the methane emissions (Fig. 2b), the methane response is only associated with the reduction in OH availability due to the higher H₂ concentration. The critical HEI is not defined for this blue H₂ as the methane burden increases in all cases. The worst scenarios of blue H₂ with 2% CH₄ leak rates show drastic differences in the tropospheric concentrations of the two gases, which increase considerably, with a weakly nonlinear effect due to the drop in atmospheric OH.

The atmospheric methane response to future H₂ production^{2,33,34} shows qualitatively similar results as a function of the H₂ production pathway and the percentage of H₂ lost to the atmosphere (Fig. 3b). Positive effects in terms of methane mitigation are observed only for green and blue H₂ with low methane losses, if the H₂ emission intensity is well below 10%. Otherwise, the tropospheric methane burden is enhanced.

We also evaluated the change in CO₂ concentration (Δ[CO₂e]) that would produce equivalent radiative forcing to the change in the equilibrium concentration of CH₄ (Figs. 2c and 3b). We used the radiative efficiency of CH₄ that includes indirect effects on O₃ and stratospheric H₂O³⁵. Under the worst scenario of blue H₂ production with 2% CH₄ losses and 10% H₂ losses, the rise in equilibrium CH₄ due to future H₂ production would be like adding 9 ppm of CO₂ to the

atmosphere (Fig. 3b). For the same blue H₂, the rise in CH₄ following the entire displacement of fossil fuels would be like adding around 70 ppm of CO₂ (Fig. 2c). This is equivalent to around 50% of the CO₂ increase from preindustrial times (278 ppm) to current days (417 ppm). Since the goal of keeping the global average temperature rise below 1.5 °C requires a mid-century maximum of CO₂ close to 450 ppm, these results support previous concerns about the sustainability of blue H₂³⁶ unless fugitive emissions can be kept sufficiently low.

Critical HEI for methane mitigation

The quantification of the critical hydrogen emission intensity (HEI_{cr}) for methane mitigation is key to assess whether displacing fossil fuels with hydrogen would mitigate or enhance the tropospheric burden of CH₄. Here we investigate how the HEI_{cr} is affected by the hydrogen production pathway and by two of the most uncertain terms in the CH₄-H₂-OH balance: (i) the partitioning of the OH sink among the tropospheric gases; (ii) the rate of H₂ uptake by soil bacteria. The derivation of an analytical solution for the HEI_{cr} is reported in the “Methods”.

The very short lifetime of OH makes the quantification of its atmospheric dynamics extremely challenging. Indirect methods are typically used to estimate OH concentrations, sources, and sink partitioning^{37–39}. Using a range of OH partition estimates^{38,40}, we investigate the dependence of the HEI_{cr} to different values of OH excess (E_{OH}), E_{OH} being the excess of OH that is consumed by other tropospheric gases besides hydrogen, methane, and carbon monoxide. Figure 4 shows the quasi-linear response of the HEI_{cr} to E_{OH} . We stress that a variation in E_{OH} is equivalent to a variation in the OH sources since we preserve the current average OH concentration, which is relatively well constrained by inverse modeling^{37,41}.

The HEI_{cr} is much lower for blue H₂ than for green H₂ because of the methane emissions associated with blue H₂ production. For the current tropospheric conditions, we find that HEI_{cr} is around 9% for green H₂, around 7% for blue H₂ with 0.2% methane leak rates, and 4.5% for blue H₂ with 0.5% methane leak rates. Blue H₂ with 1% methane leak rate has a HEI_{cr} that is close to zero, as displacement of fossil fuel with this hydrogen does not reduce methane emissions (Fig. 3b). For even higher methane leak rates, the methane burden would increase regardless of the H₂ emissions, so that the HEI_{cr} is negative.

The H₂ uptake by soil bacteria is another crucial process in the evaluation of HEI_{cr} and in the overall CH₄-H₂-OH dynamics, since it accounts for 70–80% of H₂ tropospheric removal¹¹. Despite recent research on uptake modeling^{42,43} and the microbial characterization of the H₂-oxidizing bacteria⁴⁴, the spatial heterogeneity of the uptake as driven by local hydro-climatic and biotic conditions hinders bottom-up estimates of the global average uptake rate. In atmospheric studies, the average uptake rate is usually adjusted in order to obtain a reasonable simulation of observed surface hydrogen concentrations^{14,45}.

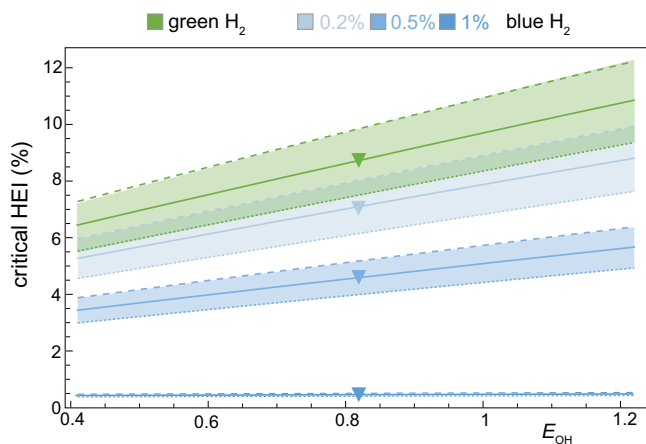


Fig. 4 | Critical hydrogen emission intensity (HEI) for methane mitigation. Critical HEI as a function of OH excess (E_{OH}) and hydrogen production method (green and blue H_2 with 0.2, 0.5, 1% CH_4 leak rates, respectively). Dashed (dotted) lines are obtained for a 20% increase (decrease) in the H_2 uptake rate by soil bacteria (k_d). Triangles mark the critical HEI for the best estimate of E_{OH} .

To account for these potential sources of uncertainties, we show how a $\pm 20\%$ variation in the uptake rate influences the critical HEI (bands in Fig. 4). A stronger biotic sink (dashed lines) reduces the consumption of OH by H_2 and, consequently, increases the HEI_{cr} . A weaker biotic sink (dotted line) has the opposite effect.

Regarding the impact of climate change on the H_2 soil sink, recent studies indicate that increasing temperatures are expected to slightly favor the uptake on a global scale¹⁴, while shifts in rainfall regimes will be the significant drivers of H_2 uptake changes at the local scale⁴³. From a biotic perspective, the adaptability of H_2 -oxidizing bacteria to extreme environments⁴⁶ suggests that their presence will remain widespread in the future, but their spatial heterogeneity may change as a result of climate and anthropogenic pressures.

Another source of uncertainties in the evaluation of HEI_{cr} is related to the estimate of CH_4 emissions associated with fossil fuel use. Since there is a quasi linear relationship between these emissions and the HEI_{cr} (Eq. (16) in “Methods”), the same relative uncertainty of fossil fuel methane emissions (Fig. 1) applies to the HEI_{cr} .

Discussion

The success of the global net-zero transition hinges on hydrogen as a scalable low-carbon energy carrier that can replace fossil fuels in several hard-to-electrify energy and transport sectors. More than 20 governments and many companies have already announced strategies for hydrogen production, and the numbers are likely to increase as policy frameworks that facilitate hydrogen adoption are promoted^{1,2}. Considerable investments are still needed to achieve such a transition, as the current hydrogen momentum falls short compared to net-zero goals. The Hydrogen Council² estimates that there is a USD 540 billion gap between the investments of announced projects (USD 160 billion) on hydrogen production and the investments required by 2030 to be on a net-zero pathway (USD 700 billion).

While the positive effects of a more hydrogen-based economy are relatively established (e.g., lower CO_2 emissions, decreased urban pollution, etc.), considerable uncertainty still surrounds the consequences of hydrogen emissions to the atmosphere, because of potential indirect GHG effects^{14,19}. Here we have focused on the impact of a more hydrogen-based energy system on tropospheric methane, the second most important greenhouse gas.

We have shown how the replacement of fossil fuel energy with green or blue hydrogen could have very different consequences for tropospheric CH_4 , depending on the amount of hydrogen lost to the

atmosphere and the methane emissions associated with hydrogen production (Figs. 2 and 3). Specifically, tropospheric CH_4 would decrease due to the fossil fuel displacement only if the rate of H_2 losses is kept below the critical HEI.

This is around $9 \pm 3\%$ for green H_2 (Fig. 4). The same critical value would apply to other H_2 colors that do not entail the use of fossil fuels, like white or orange H_2 extracted from underground deposits^{12,47}. The critical HEI for blue H_2 is much lower due to the CH_4 emission associated with blue H_2 production. We have found that the methane emissions in a blue H_2 economy could be higher than in a fossil fuel economy if the methane supply chain had an average leak rate above 1%. Furthermore, the superimposition of CH_4 and H_2 emissions may have undesired consequences for the tropospheric burden of CH_4 . This may be a potential problem in the near term, given that steam methane reforming will be used to bridge the gap between increasing H_2 demand and limited green H_2 production capacities². Our results suggest that including hydrogen emissions would aggravate the greenhouse gas footprint of blue H_2 ³⁶.

In addition to the CH_4 feedback, H_2 emissions are also expected to impact ozone (O_3) and stratospheric water vapor (H_2O), with negative consequences for both air quality and radiative forcing. Accounting for these effects, we can provide a comparison between the radiative forcing of hydrogen-based and fossil fuel-based energy systems. Because both H_2 and CH_4 are short-lived gas compared to CO_2 , the time horizon for this comparison is crucial⁴⁸. Here we consider 20-year and 100-year time horizons. The GWP of H_2 is estimated at 11 ± 5 (100-year) and 33^{+11}_{-13} (20-year)¹⁶. The GWP of CH_4 is estimated at 28 (100-year) and 80 (20-year)³⁵. In an envisioned hydrogen economy that replaces the current fossil fuel industry, the H_2 emissions could be in the range 23 to 370 Tg H_2 yr⁻¹, for a H_2 emission intensity going from 1 to 10% (Fig. 2a). These emissions would have a radiative forcing impact of 0.7–12% (100-year) and 2–35% (20-year) of the current CO_2 emissions from fossil fuels (≈ 35 Pg CO_2 yr⁻¹). If the global H_2 economy relied on blue H_2 with a 2% methane leakage rate, methane emissions would cause an additional radiative forcing impact that is around 10% (100-year) and 27% (20-year) of the current CO_2 emissions from fossil fuels. Hence, in the worst scenario, up to 22% of the climate benefits of the hydrogen economy could be offset by gas losses over a 100-year horizon. The percentage could be as large as 65% over a 20-year horizon. These values could be higher on a regional scale if the leak rate of the natural gas supply chain is above 2%.

To maximize the climate benefit of hydrogen adoption, minimizing both H_2 and CH_4 losses across the supply chain of hydrogen production will need to be a priority. On the methane side, some governments and companies have already committed to reducing the leaks from the oil and gas sector, because this could be the most cost-effective and impactful action for near-term climate mitigation²¹. The International Energy Agency (IEA) estimates that, with the recent rise in natural gas prices, the abatement of methane emissions from the global gas and oil sector could be implemented at no net cost⁴⁹. Hence, the accomplishment of this mitigation is only a matter of political will for the limited number of companies involved.

On the hydrogen side, the global value chain still has to be built. This offers the advantage of tackling the hydrogen emission problem ahead of time. On the one hand, energy companies will have a great interest in minimizing economic loss and safety risks due to hydrogen leaks. On the other hand, however, many technological challenges still need to be addressed. First, H_2 containment may remain an issue even as technologies progress. The high diffusivity of the small H_2 molecule has already challenged the scientific community’s ability to measure the H_2 concentration in the atmosphere⁵⁰ and in the firm air of ice sheets⁵¹. Second, while more field-based estimates of H_2 losses are needed, there is currently no commercially available sensing technology able to detect small H_2 leaks at the ppb level⁴⁸. Third, global-space monitoring, which is bringing a much-needed transparency to the

quantification of real methane emissions^{27,31}, will also require new technology since H₂, unlike CH₄ or CO₂, does not absorb infrared radiation. For all these reasons, the uncertainty about future emissions from the H₂ value chain remains large.

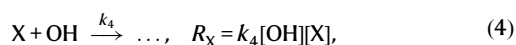
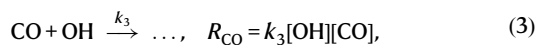
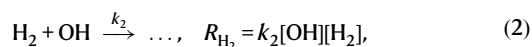
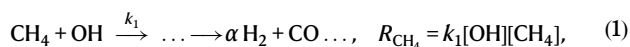
Our versatile atmospheric model allowed a broad exploration of scenarios in a hydrogen-based energy system. Simulations with high resolution three-dimensional atmospheric chemistry models, which are more comprehensive but more computationally demanding, could refine our results for specific scenarios. In particular, a more detailed model could improve the assessment of H₂ displacement of fossil fuels by accounting for the emission changes of other chemical species, like CO and NO_x, which impact the CH₄-H₂-OH dynamics. Further analyses could also refine the potential changes in emission inventories due to H₂ displacement of different fossil fuels.

Methods

The Model

With the increasing anthropogenic alteration of atmospheric chemistry, detailed three-dimensional atmospheric chemistry models have become critical to evaluate the atmospheric interactions with the climate forcing^{52,53}. Nonetheless, thanks to their versatility, simplified models of atmospheric chemistry have also proven very useful to investigate the fundamental processes governing the coupling between atmospheric gases and the consequences of their possible perturbations (e.g., refs. 54–59). The insights obtained with the CH₄-CO-OH model by Prather et al.⁵⁴, in particular, led to a +40% revision of the IPCC's GWP for CH₄⁶⁰. Here we extend Prather's seminal model by adding the mass balance equation for atmospheric H₂. The purpose is to identify the key components that control the H₂ feedback on the tropospheric dynamics of CH₄ (Fig. 1).

The chemical reactions considered are



with R representing the rates of reactions, $[\cdot]$ the concentrations, and k_i the rate coefficients. We indicated only the products with which we are concerned, the CO and H₂ produced by oxidation of CH₄(1). H₂

production through CH₄ oxidation has yield $\alpha \approx 0.37^{13}$. X encompasses all the other species, besides CH₄, CO, and H₂, that consume OH. Based on the above reactions, the balance equations for the CH₄-H₂-CO-OH system are

$$\frac{d[\text{CH}_4]}{dt} = S_{\text{CH}_4} - R_{\text{CH}_4} - R_s, \quad (5)$$

$$\frac{d[\text{H}_2]}{dt} = S_{\text{H}_2} + \alpha R_{\text{CH}_4} - R_{\text{H}_2} - R_d, \quad (6)$$

$$\frac{d[\text{CO}]}{dt} = S_{\text{CO}} + R_{\text{CH}_4} - R_{\text{CO}}, \quad (7)$$

$$\frac{d[\text{OH}]}{dt} = S_{\text{OH}} - R_{\text{CH}_4} - R_{\text{H}_2} - R_{\text{CO}} - R_X, \quad (8)$$

where $R_d = k_d[\text{H}_2]$ is the H₂ uptake by soil bacteria, which plays a crucial role in the global balance of H₂ since it accounts for around 70–80% of tropospheric removal^{11,43,61}; $R_s = k_s[\text{CH}_4]$ accounts for the smaller sinks of CH₄, namely soil uptake, stratospheric loss and reactions with chlorine radicals⁶². For simplicity, we neglect the smaller sinks of H₂, i.e., stratospheric loss ($\approx 1\%$ of removal⁶³), and CO, i.e., soil uptake and stratospheric loss ($<10\%$ of removal⁶⁴).

The solution at quasi steady state (i.e., $d[\cdot]/dt = 0$) provides the sources for fixed tropospheric concentrations. Positive solutions for OH occurs if $S_{\text{OH}} > (2 + \alpha)(S_{\text{CH}_4} - R_s) + S_{\text{CO}} + S_{\text{H}_2} - R_d$, i.e., when there is enough OH to oxidize all CO sources, the part of CH₄ sources that is not balanced by smaller sinks, and the part of H₂ sources that is not balanced by the soil uptake. The excess of OH consumed by other gases, besides CH₄, CO, and H₂, can be defined as $E_{\text{OH}} = R_X / (R_{\text{CH}_4} + R_{\text{CO}} + R_{\text{H}_2})$. The values representing average tropospheric conditions are summarized in Table 1. The values of S_{OH} and S_{CO} are kept constant in all scenarios.

Linear stability and transient dynamics

We investigate the effects of an emission pulse of H₂ on the tropospheric system (5)–(8). The timescales and modes of the atmospheric response to chemical perturbations are defined by the eigenvalues and eigenvectors of the system^{54,55}. Indicating with $\mathbf{c}(t)$ the solution vector of the system (5)–(8), the temporal dynamics of a small perturbation $\hat{\mathbf{c}}$ around \mathbf{c} evolves as

$$\frac{d\hat{\mathbf{c}}}{dt} = \mathbf{J}\hat{\mathbf{c}}, \quad (9)$$

Table 1 | Tropospheric budgets of key species and definition of linear stability modes

		CH ₄	H ₂	CO	OH	$-\lambda_i^{-1}(\text{yr})$
Steady state	Concentration (ppb)	1890	530	80	10 ⁶ cm ⁻³	
	Sources (ppb/yr)	226	265 ^a	480 ^a	1333	
	τ (yr)	8.3	2	0.17	1 s	
Linear stability	CH ₄ mode	1%	0.31%	0.64%	-0.39%	12.3
	H ₂ mode	-0.01%	1%	0.03%	-0.06%	2
	CO mode	-0.008%	0.001%	1%	-0.36%	0.2
	OH mode	... ^b	... ^b	... ^b	1%	1.5 s

^aSources for CO and H₂ include production from CH₄ oxidation.

^b... is $<10^{-7}$.

Sources are obtained from the system (5)–(8) at steady state with the current tropospheric concentrations. τ is the average lifetime of each gas. The modes are expressed as relative changes normalized so that the dominant species' ratio is 1%. Reaction rates are defined as follows: $k_1 = 3.17 \times 10^{-15}$ cm³/s; $k_2 = 3.8 \times 10^{-15}$ cm³/s; $k_3 = 1.9 \times 10^{-13}$ cm³/s; $k_s = 0.02$ yr⁻¹; $k_d = 0.38$ yr⁻¹ is such that soil uptake accounts for 75% of atmospheric H₂ removal; $k_4[\text{X}] = 0.3$ s⁻¹ ($E_{\text{OH}} = 0.82$) is defined so that 45% of OH is consumed by the species X, 36% by CO, 14% by CH₄, and 5% by H₂³⁸. Concentrations are converted to mixing ratios using 1 ppb = 1.57×10^{10} cm⁻³; sources are converted from ppb/yr to Tg/yr using 4.22×10^{18} kg as the troposphere mass⁶⁸.

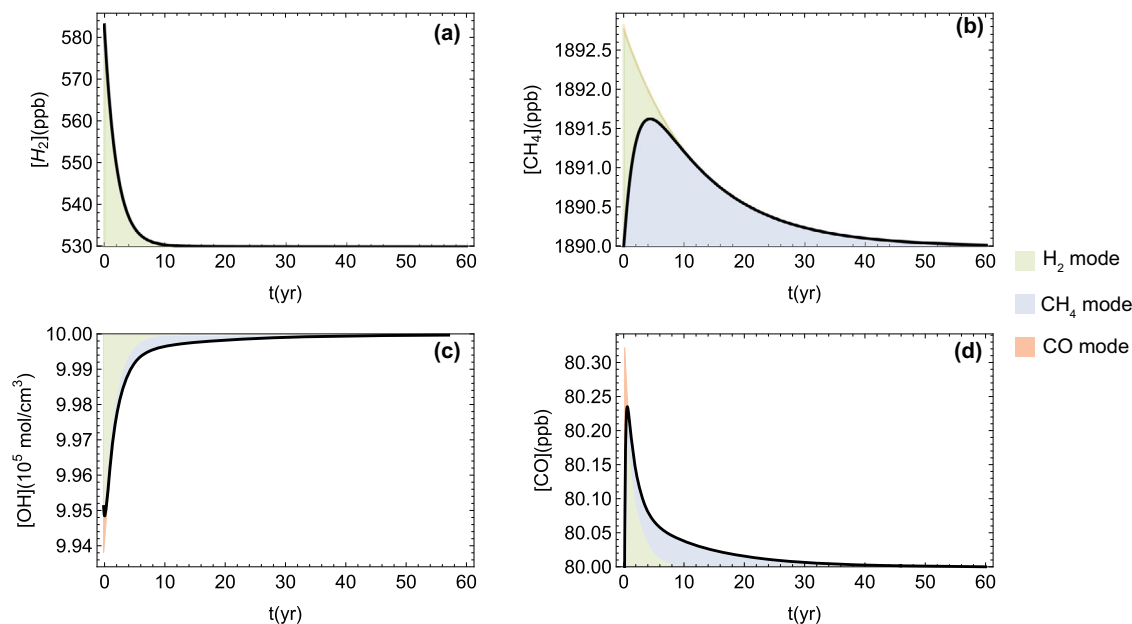


Fig. 5 | Transient dynamics. Tropospheric response to a pulse of H₂ (10% increase of its concentration). Temporal dynamics of H₂ (a), CH₄ (b), OH (c), and CO (d).

Colors highlight the contributions of the different modes. When different modes superimpose, the faster-decaying mode is shown on top of the others.

where **J** is the Jacobian of the system evaluated in **c**. For the equilibrium solution **c**₀ representing the current tropospheric concentrations, the eigenvalues and eigenvectors, or modes, of the linearized system (9) are reported in Table 1. Since all eigenvalues are real and negative ($\lambda_i < 0$), the equilibrium solution **c**₀ is a stable node. As a result, any small perturbation asymptotically decays in time with a timescale defined by the negative reciprocal of the eigenvalue.

Because the system equations are coupled, the decay timescale ($-\lambda_i^{-1}$) of a gas perturbation does not necessarily correspond to the gas steady state average lifetime (τ_i). The CH₄ perturbation, in particular, decays with a timescale that is much larger than what predicted by its steady state lifetime, i.e., $R = -\lambda_{\text{CH}_4}^{-1} / \tau_{\text{CH}_4} > 1$. This mechanism, known as the CH₄ feedback effect^{55,65}, has a crucial role in increasing the GWP and the environmental impact of CH₄ emissions. Detailed models of atmospheric chemistry usually provide *R* around 1.3–1.4⁶⁵. We find a marginally higher feedback factor, namely $R \approx 1.5$, in agreement with previous findings using Prather’s box model^{54,55,57}. The decay timescale of the H₂ perturbation instead corresponds to the H₂ average lifetime, namely $-\lambda_{\text{H}_2}^{-1} \approx \tau_{\text{H}_2}$, in agreement with results from detailed atmospheric chemistry models¹⁹.

While the modal eigenvalue analysis correctly captures the asymptotic stability of the solution **c**₀, it does not describe the perturbation dynamics at finite times, i.e., before the asymptotic decay. Still within the domain of the linearized system (9), a more complete picture can be obtained by analyzing the temporal evolution of the solutions with specific attention to the emergence of transient growth phenomena, which are known to occur in systems where the modes are non-orthogonal, as in the present case. When large enough, a transient growth can even trigger nonlinearities that destabilize the equilibrium solution⁶⁶.

Figure 5 shows the transient growth phase of tropospheric CH₄ and CO that follows a 10% perturbation of H₂ concentration. Specifically, the pulse of H₂ causes a drop in OH and a build-up of CH₄ that lasts a few years, while the H₂ perturbation decays with the timescale τ_{H_2} . The CH₄ build-up then decays in the same manner as would a direct pulse of CH₄ with a timescale defined by the CH₄ feedback effect. In analytical terms, the perturbation of tropospheric CH₄ mainly

due to the excitation of H₂ and CH₄ modes is given by $\delta[\text{CH}_4] \approx 2.76e^{\lambda_{\text{CH}_4} t} - 2.82e^{\lambda_{\text{H}_2} t} + 0.06e^{\lambda_{\text{CO}} t}$.

Using this result in traditional GWP formulas³⁵ yields a GWP for H₂ due to direct CH₄ perturbation around 7.8 with the 100-year time-horizon and 22 with the 20-year time horizon. It is estimated that around half of the H₂ indirect radiative forcing is due to the direct CH₄ perturbation, and the other half to the O₃ and stratospheric H₂O impacts caused by both H₂ and H₂-induced CH₄ perturbations¹⁴. Taking this into account yields a total GWP for H₂ of 15.6 with the 100-year time-horizon and 44 with the 20-year time-horizon. These values are in the upper range of the recent estimates of 11 ± 5 for GWP100 and 33^{+11}_{-13} for GWP20 obtained with a detailed model of atmospheric chemistry¹⁶. Notably, the consequences of the H₂ pulse on CH₄ are relatively small in magnitude because most of the additional H₂ is oxidized by soil bacteria and not by OH. The stability of this biotic sink as affected by climate change and anthropic pressure is hence a crucial aspect for the impact of future H₂ emissions, as further discussed in the main text.

Critical hydrogen emission intensity

We here derive an explicit expression for the critical H₂ emission intensity (HEI_{cr}) for methane mitigation, defined as the emission rate that offsets the H₂ replacement of fossil fuels. The expression is derived for an infinitesimal replacement of fossil fuel energy with H₂ (dE in ExJ/yr), but well approximates the critical HEI for finite replacement of fossil fuel energy (see Supplementary Fig. 3). As a first step, we differentiate the system (5)–(8) at equilibrium ($d[\cdot]/dt = 0$) with respect to *E*. This yields

$$S_{\text{CH}_4, E} - k_1[\text{CH}_4][\text{OH}]_E = 0, \quad (10)$$

$$S_{\text{H}_2, E} + \alpha k_1[\text{CH}_4][\text{OH}]_E - k_2([\text{H}_2][\text{OH}]_E) - k_d[\text{H}_2]_E = 0, \quad (11)$$

$$k_1[\text{CH}_4][\text{OH}]_E - k_3([\text{CO}][\text{OH}]_E) = 0, \quad (12)$$

$$k_1[\text{CH}_4][\text{OH}]_E + k_2([\text{H}_2][\text{OH}]_E) + k_3([\text{CO}][\text{OH}]_E) + k_4[\text{X}][\text{OH}]_E = 0, \quad (13)$$

where subscript E indicates $d \cdot /dE$. $[\text{CH}_4]_E = 0$ because of the definition of the critical H_2 emission intensity, which leaves the methane concentration unaltered. We consider that only H_2 and CH_4 sources vary with E , while $S_{\text{OH},E} = S_{\text{CO},E} = 0$. These variations can be estimated as

$$S_{\text{H}_2,E} = a_{\text{H}_2} \left(-\text{ff}_{\text{H}_2} + \frac{\text{HEI}}{\eta_{\text{H}_2}(1 - \text{HEI})} \right), \quad (14)$$

$$S_{\text{CH}_4,E} = a_{\text{CH}_4} \left(-\text{ff}_{\text{CH}_4} + \frac{r \text{MEI}}{\eta_{\text{H}_2}(1 - \text{HEI})} \right), \quad (15)$$

where HEI and MEI are the hydrogen and methane emission intensities, respectively (MEI = 0 for green H_2); η_{H_2} is H_2 higher heating value; r is the amount of CH_4 needed to produce a unit of blue H_2 ; ff_{CH_4} and ff_{H_2} are the average amounts of CH_4 and H_2 emitted per ExJ of fossil fuel energy; a_{H_2} and a_{CH_4} are conversion factors.

Substituting Eqs. (14), (15) into the system (10)–(13) and after some algebra, one obtains the critical H_2 emission intensity

$$\text{HEI}_{\text{cr}} = \frac{A(\text{ff}_{\text{CH}_4} \eta_{\text{H}_2} - r \text{MEI}) + B \text{ff}_{\text{H}_2} \eta_{\text{H}_2}}{A \text{ff}_{\text{CH}_4} \eta_{\text{H}_2} + B(\text{ff}_{\text{H}_2} \eta_{\text{H}_2} + 1)}. \quad (16)$$

where the dependence to the atmospheric composition is embedded in $A = k_d(k_4[X] + k_2[\text{H}_2] + 2k_1[\text{CH}_4]) + k_2[\text{OH}](\alpha + 2)k_1[\text{CH}_4] + k_4[X]$ and $B = 8k_1k_2[\text{CH}_4][\text{OH}]$. Parameters have been defined as follows: $\eta_{\text{H}_2} = 0.143 \text{ ExJ/Tg}_{\text{H}_2}$, $r = 3.2 \text{ kg}_{\text{CH}_4}/\text{kg}_{\text{H}_2}$, $\text{ff}_{\text{CH}_4} = 0.225 \text{ Tg}_{\text{CH}_4}/\text{ExJ}$, $\text{ff}_{\text{H}_2} = 0.0225 \text{ Tg}_{\text{H}_2}/\text{ExJ}$, $a_{\text{CH}_4} = 0.43 \text{ ppb/Tg}$, $a_{\text{H}_2} = 8a_{\text{CH}_4}$. To obtain the value of r , we used the estimate of 3.7 kg of natural gas for kg of H_2 ⁶⁷, which includes feedstock and energy requirements, and we assumed that 85% of natural gas by weight is composed by methane. ff_{CH_4} and ff_{H_2} are obtained as the ratio between the global CH_4 and H_2 emissions due to fossil fuel use and the global fossil fuel energy.

Data availability

All data generated during this study are provided in the supplementary dataset file.

Code availability

The code used to generate the results is provided in the supplementary dataset file.

References

1. IEA. *Global Hydrogen Review*. Technical Report (International Energy Agency, 2021).
2. Hydrogen Council. *Hydrogen for Net-Zero: A Critical Cost-Competitive Energy Vector*. Technical Report (European Union, 2021).
3. Wang, D. et al. Impact of a future H_2 -based road transportation sector on the composition and chemistry of the atmosphere—part 1: tropospheric composition and air quality. *Atmos. Chem. Phys.* **13**, 6117–6137 (2013).
4. van Ruijven, B., Lamarque, J.-F., van Vuuren, D. P., Kram, T. & Eerens, H. Emission scenarios for a global hydrogen economy and the consequences for global air pollution. *Glob. Environ. Change* **21**, 983–994 (2011).
5. Frazer-Nash Consultancy. *Fugitive Hydrogen Emissions in a Future Hydrogen Economy*. Technical Report (Frazer-Nash Consultancy, 2022).
6. Cooper, J., Dubey, L., Bakkaloglu, S. & Hawkes, A. Hydrogen emissions from the hydrogen value chain-emissions profile and impact to global warming. *Sci. Total Environ.* **830**, 154624 (2022).
7. Derwent, R. G., Collins, W. J., Johnson, C. & Stevenson, D. Transient behaviour of tropospheric ozone precursors in a global 3-D CTM and their indirect greenhouse effects. *Climatic Change* **49**, 463–487 (2001).
8. Tromp, T. K., Shia, R.-L., Allen, M., Eiler, J. M. & Yung, Y. L. Potential environmental impact of a hydrogen economy on the stratosphere. *Science* **300**, 1740–1742 (2003).
9. Schultz, M. G., Diehl, T., Brasseur, G. P. & Zittel, W. Air pollution and climate-forcing impacts of a global hydrogen economy. *Science* **302**, 624–627 (2003).
10. Warwick, N., Bekki, S., Nisbet, E. & Pyle, J. Impact of a hydrogen economy on the stratosphere and troposphere studied in a 2-d model. *Geophys. Res. Lett.* **31**, p.L05107 (2004).
11. Ehalt, D. H. & Rohrer, F. The tropospheric cycle of H_2 : a critical review. *Tellus B: Chem. Phys. Meteorol.* **61**, 500–535 (2009).
12. Zgonnik, V. The occurrence and geoscience of natural hydrogen: a comprehensive review. *Earth-Sci. Rev.* **203**, 103140 (2020).
13. Novelli, P. C. et al. Molecular hydrogen in the troposphere: global distribution and budget. *J. Geophys. Res.: Atmospheres* **104**, 30427–30444 (1999).
14. Paulot, F. et al. Global modeling of hydrogen using GFDL-AM4.1: sensitivity of soil removal and radiative forcing. *Int. J. Hydrog. Energy* **46**, 13446–13460 (2021).
15. Vogel, B., Feck, T., Grob, J.-U. & Riese, M. Impact of a possible future global hydrogen economy on Arctic stratospheric ozone loss. *Energy Environ. Sci.* **5**, 6445 (2012).
16. Warwick, N. et al. *Atmospheric Implications of Increased Hydrogen Use*. Technical Report (Department for Business, Energy & Industrial Strategy Policy Paper, 2022).
17. Kirschke, S. et al. Three decades of global methane sources and sinks. *Nat. Geosci.* **6**, 813–823 (2013).
18. Saunio, M. et al. The global methane budget 2000–2017. *Earth Syst. Sci. Data* **12**, 1561–1623 (2020).
19. Derwent, R. G. et al. Global modelling studies of hydrogen and its isotopomers using STOCHEM-CRI: Likely radiative forcing consequences of a future hydrogen economy. *Int. J. Hydrog. Energy* **45**, 9211–9221 (2020).
20. Patterson, J. D. et al. Atmospheric history of H_2 over the past century reconstructed from south pole firn air. *Geophys. Res. Lett.* **47**, e2020GL087787 (2020).
21. European Commission. Launch by the United States, the European Union, and Partners of the Global Methane Pledge to Keep 1.5C Within Reach. https://ec.europa.eu/commission/presscorner/detail/en/statement_21_5766. Accessed 2021-11-30 (2021).
22. BP. *Statistical Review of World Energy*. Technical Report (British Petroleum, 2021).
23. Bond, S., Gül, T., Reimann, S., Buchmann, B. & Wokaun, A. Emissions of anthropogenic hydrogen to the atmosphere during the potential transition to an increasingly H_2 -intensive economy. *Int. J. Hydrog. Energy* **36**, 1122–1135 (2011).
24. Schwietzke, S. et al. Upward revision of global fossil fuel methane emissions based on isotope database. *Nature* **538**, 88–91 (2016).
25. Jackson, R. B. et al. Increasing anthropogenic methane emissions arise equally from agricultural and fossil fuel sources. *Environ. Res. Lett.* **15**, 071002 (2020).
26. IEA. *Global Methane Tracker 2022*. Technical Report (International Energy Agency, 2022).
27. Zhang, Y. et al. Quantifying methane emissions from the largest oil-producing basin in the united states from space. *Sci. Adv.* **6**, 5120 (2020).
28. Alvarez, R. A. et al. Assessment of methane emissions from the U.S. oil and gas supply chain. *Science* **361**, 186–188 (2018).
29. Shen, L. et al. Satellite quantification of oil and natural gas methane emissions in the U.S. and Canada including contributions from

- individual basins. *Atmos. Chem. Phys. Discuss.* **22**, 11203–11215 (2022).
30. MacKay, K. et al. Methane emissions from upstream oil and gas production in Canada are underestimated. *Sci. Rep.* **11**, 1–8 (2021).
31. Lauvaux, T. et al. Global assessment of oil and gas methane ultra-emitters. *Science* **375**, 557–561 (2022).
32. UNEP. *An Eye on Methane: International Methane Emissions Observatory*. Technical Report (United Nations Environment Program, 2021).
33. IEA. *Net Zero by 2050 - A Roadmap for the Global Energy Sector*. Technical Report (International Energy Agency, 2021).
34. IRENA. *World Energy Transitions Outlook: 1.5° C Pathway*. Technical Report (International Renewable Energy Agency, 2021).
35. Forster, P. et al. *Climate Change 2021: The Physical Science Basis. Contribution of Working Group I to the Fifth Assessment Report of the Intergovernmental Panel on Climate Change* Chap. 7 (Cambridge University Press, 2021).
36. Howarth, R. W. & Jacobson, M. Z. How green is blue hydrogen? *Energy Sci. Eng.* **9**, 1676–1687 (2021).
37. Naik, V. et al. Preindustrial to present-day changes in tropospheric hydroxyl radical and methane lifetime from the Atmospheric Chemistry and Climate Model Intercomparison Project (ACCMIP). *Atmos. Chem. Phys.* **13**, 5277–5298 (2013).
38. Lelieveld, J., Gromov, S., Pozzer, A. & Taraborrelli, D. Global tropospheric hydroxyl distribution, budget, and reactivity. *Atmos. Chem. Phys.* **16**, 12477–12493 (2016).
39. Murray, L. T., Fiore, A. M., Shindell, D. T., Naik, V. & Horowitz, L. W. Large uncertainties in global hydroxyl projections tied to fate of reactive nitrogen and carbon. *Proc. Natl Acad. Sci. USA* **118**, e2115204118 (2021).
40. Warneck, P. *Chemistry of the Natural Atmosphere* (Elsevier, 1999).
41. Montzka, S. A. et al. Small interannual variability of global atmospheric hydroxyl. *Science* **331**, 67–69 (2011).
42. Ehhalt, D. & Rohrer, F. Deposition velocity of H₂: a new algorithm for its dependence on soil moisture and temperature. *Tellus B: Chem. Phys. Meteorol.* **65**, 19904 (2013).
43. Bertagni, M. B., Paulot, F. & Porporato, A. Moisture fluctuations modulate abiotic and biotic limitations of soil H₂ uptake. *Global Biogeochem. Cycles* **35**, e2021GB006987 (2021).
44. Bay, S. K. et al. Trace gas oxidizers are widespread and active members of soil microbial communities. *Nat. Microbiol.* **6**, 246–256 (2021).
45. Yashiro, H., Sudo, K., Yonemura, S. & Takigawa, M. The impact of soil uptake on the global distribution of molecular hydrogen: chemical transport model simulation. *Atmos. Chem. Phys.* **11**, 6701–6719 (2011).
46. Ji, M. et al. Atmospheric trace gases support primary production in Antarctic desert surface soil. *Nature* **552**, 400–403 (2017).
47. Osselin, F. et al. Orange hydrogen is the new green. *Nat. Geosci.* **15**, 1–5 (2022).
48. Ocko, I. B. & Hamburg, S. P. Climate consequences of hydrogen emissions. *Atmos. Chem. Phys.* **22**, 9349–9368 (2022).
49. IEA. *Driving Down Methane Leaks from the Oil and Gas Industry*. Technical Report (International Energy Agency, 2021).
50. Jordan, A. & Steinberg, B. Calibration of atmospheric hydrogen measurements. *Atmos. Meas. Tech.* **4**, 509–521 (2011).
51. Patterson, J. D. & Saltzman, E. S. Diffusivity and solubility of H₂ in ice Ih: implications for the behavior of H₂ in polar ice. *J. Geophys. Res.: Atmos.* **126**, 2020–033840 (2021).
52. Lamarque, J.-F. et al. The atmospheric chemistry and climate model intercomparison project (ACCMIP): overview and description of models, simulations, and climate diagnostics. *Geosci. Model Dev.* **6**, 179–206 (2013).
53. Shindell, D. T. et al. Radiative forcing in the ACCMIP historical and future climate simulations. *Atmos. Chem. Phys.* **13**, 2939–2974 (2013).
54. Prather, M. J. Lifetimes and eigenstates in atmospheric chemistry. *Geophys. Res. Lett.* **21**, 801–804 (1994).
55. Prather, M. J. Time scales in atmospheric chemistry: theory, GWPs for CH₄ and CO, and runaway growth. *Geophys. Res. Lett.* **23**, 2597–2600 (1996).
56. Manning, M. R. Characteristic modes of isotopic variations in atmospheric chemistry. *Geophys. Res. Lett.* **26**, 1263–1266 (1999).
57. Prather, M. J. Lifetimes and time scales in atmospheric chemistry. *Philos. Trans. R. Soc. A: Math., Phys. Eng. Sci.* **365**, 1705–1726 (2007).
58. Gaubert, B. et al. Chemical feedback from decreasing carbon monoxide emissions. *Geophys. Res. Lett.* **44**, 9985–9995 (2017).
59. Heimann, I. et al. Methane emissions in a chemistry-climate model: Feedbacks and climate response. *J. Adv. Modeling Earth Syst.* **12**, 2019–002019 (2020).
60. Houghton, J. T. et al. *Climate Change 2001: The Scientific Basis* (The Press Syndicate of the University of Cambridge, 2001).
61. Rhee, T. S., Brenninkmeijer, C. A. M. & Rockmann, T. The overwhelming role of soils in the global atmospheric hydrogen cycle. *Atmos. Chem. Phys.* **6**, 1611–1625 (2006).
62. Prather, M. J., Holmes, C. D. & Hsu, J. Reactive greenhouse gas scenarios: Systematic exploration of uncertainties and the role of atmospheric chemistry. *Geophys. Res. Lett.* **39**, L09803 (2012).
63. Xiao, X. et al. Optimal estimation of the soil uptake rate of molecular hydrogen from the Advanced Global Atmospheric Gases Experiment and other measurements. *J. Geophys. Res.: Atmos.* <https://doi.org/10.1029/2006JD007241> (2007).
64. Zheng, B. et al. Global atmospheric carbon monoxide budget 2000–2017 inferred from multi-species atmospheric inversions. *Earth Syst. Sci. Data* **11**, 1411–1436 (2019).
65. Holmes, C. D. Methane feedback on atmospheric chemistry: methods, models, and mechanisms. *J. Adv. Modeling Earth Syst.* **10**, 1087–1099 (2018).
66. Schmid, P. J. Nonmodal stability theory. *Annu. Rev. Fluid Mech.* **39**, 129–162 (2007).
67. Collodi, G., Azzaro, G., Ferrari, N. & Santos, S. Techno-economic evaluation of deploying ccs in SMR based merchant H₂ production with NG as feedstock and fuel. *Energy Proc.* **114**, 2690–2712 (2017).
68. Trenberth, K. E. & Smith, L. The mass of the atmosphere: a constraint on global analyses. *J. Clim.* **18**, 864–875 (2005).

Acknowledgements

We acknowledge support from the US National Science Foundation (NSF) grant nos. EAR1331846 and EAR-1338694, the BP through the Carbon Mitigation Initiative (CMI) at Princeton University, and the Moore Foundation. We thank Larry Horowitz for critical reading of the manuscript.

Author contributions

M.B.B., S.W.P., and A.P. conceptualized the work. M.B.B. developed the analytical model with contributions from F.P., analyzed the results and prepared the manuscript. A.P., F.P., and S.W.P. supervised the work and edited the manuscript.

Competing interests

The authors declare no competing interests.

Additional information

Supplementary information The online version contains supplementary material available at <https://doi.org/10.1038/s41467-022-35419-7>.

Correspondence and requests for materials should be addressed to Matteo B. Bertagni.

Peer review information *Nature Communications* thanks Jasmin Cooper and the other, anonymous, reviewer(s) for their contribution to the peer review of this work. Peer reviewer reports are available.

Reprints and permissions information is available at <http://www.nature.com/reprints>

Publisher's note Springer Nature remains neutral with regard to jurisdictional claims in published maps and institutional affiliations.

Open Access This article is licensed under a Creative Commons Attribution 4.0 International License, which permits use, sharing, adaptation, distribution and reproduction in any medium or format, as long as you give appropriate credit to the original author(s) and the source, provide a link to the Creative Commons license, and indicate if changes were made. The images or other third party material in this article are included in the article's Creative Commons license, unless indicated otherwise in a credit line to the material. If material is not included in the article's Creative Commons license and your intended use is not permitted by statutory regulation or exceeds the permitted use, you will need to obtain permission directly from the copyright holder. To view a copy of this license, visit <http://creativecommons.org/licenses/by/4.0/>.

© The Author(s) 2022